J. Phycol. **45,** 1270–1277 (2009)
© 2009 Phycological Society of America
DOI: 10.1111/j.1529-8817.2009.00755.x

THE CONCHOCELIS OF *PORPHYRA HAITANENSIS* (RHODOPHYTA) IS PROTECTED FROM HARMFUL UV RADIATION BY THE COVERING CALCAREOUS MATRIX[1]

Hongxia Jiang

State Key Laboratory of Marine Environmental Science, Xiamen University, Xiamen, Fujian, 361005, China
Department of Biology and Food Technology, Changshu Institute of Technology, Changshu, Jiangsu, 215500, China

Kunshan Gao[2]

State Key Laboratory of Marine Environmental Science, Xiamen University, Xiamen, Fujian, 361005, China

and E. Walter Helbling

Estación de Fotobiología Playa Unión and Consejo Nacional de Investigaciones Científicas y Técnicas (CONICET), Casilla de Correos N° 15 - (9103) Rawson, Chubut, Argentina

Previous study has shown that *Porphyra* conchocelis is sensitive to high levels of PAR (400–700 nm) as well as ultraviolet radiation (UVR: 280–400 nm), resulting in high inhibition of photosynthesis. However, little is known about whether the inner covering layer of the shell, in which the conchocelis lives, may provide protection against solar UVR. Our study indicates that the covering calcareous matrix is about 0.06 mm thick, transmitting 63, 47, and 28% of PAR, ultraviolet radiation A (UVA: 315–400 nm), and ultraviolet radiation B (UVB: 280–315 nm), respectively. We used a shading layer that simulated the above transmissions, and the effective quantum yield of PSII and photosynthetic carbon fixation in the conchocelis increased to greater extents in the presence of UVA or UVB. Attenuation of UVA by 19% and UVB by 37% due to the shading layer increased the PSII yield by 44%–77% and photosynthetic carbon fixation by about 60%. Our study clearly shows that the photosynthetic machinery of *Porphyra haitanensis* T. J. Chang et B. F. Zheng conchocelis was efficiently protected from harmful UVR by the covering calcareous matrix.

Key index words: **carbon fixation; conchocelis; effective quantum yield; *Porphyra haitanensis*; UVR**

Abbreviations: **MAAs, mycosporine-like amino acids; PA, PAR + UVA; PAB, PAR + UVA + UVB; UVA, ultraviolet radiation A; UVB, ultraviolet radiation B; UVR, ultraviolet radiation**

Macroalgae have gained defensive mechanisms to minimize UV-induced damage during their evolution. They are known to be able to repair UV-induced DNA damage by photoreactivation and nucleotide excision repair (Pakker et al. 2000, Lud et al. 2001) and to be capable of synthesizing and accumulating UV-absorbing compounds, such as mycosporine-like amino acids (MAAs) and phlorotannin, to screen out harmful UVR (Karsten et al. 1998, Fairhead et al. 2006). However, such defensive mechanisms against UVR (280–400 nm) seem to vary among different life-cycle stages of macroalgae. Early developmental stages are more sensitive to UVR than adult ones (Dring et al. 1996, Coelho et al. 2001), mainly because of their simpler structure that allows easier penetration of UVR. In *Porphyra*, the conchocelis stage possesses negligible amounts of MAAs and simpler structure as compared with the thallus stage, and its photosynthesis was more inhibited by UVR in the former than in the latter when exposed to solar radiation (Jiang and Gao 2008).

The life history of the genus *Porphyra* is characterized by the alternation of the microscopic conchocelis phase (the sporophyte) and a macroscopic thallus phase (the gametophyte) (Drew 1949, Cole and Conway 1980). The gametophytic phase reproduces sexually through fertilization of the carpogonium by the spermatium (Hawkes 1978), and the subsequently released zygotospores get attached to shells and develop into conchocelis in their inner layers. Shells with *Porphyra* conchocelis occur at different depths during sea-farming practice or in natural coastal waters where the alga is distributed. However, it is unknown how thick the covering calcareous matrix that shelters the conchocelis is and if it would play a protective role against solar UV radiation.

The aim of this study was to investigate the relationship of the shell cover layer and photosynthesis of *P. haitanensis* conchocelis. *P. haitanensis* is endemic to the southern part of China and is

[1]Received 25 March 2009. Accepted 12 June 2009.
[2]Author for correspondence: e-mail ksgao@xmu.edu.cn.

commercially cultivated. We hypothesized that the covering calcareous matrix can reduce the transmission of solar UVR to a significant extent, enough to protect the conchocelis from being harmed and therefore to result in higher photosynthetic performance.

MATERIALS AND METHODS

Plant materials and maintenance. Shells with their inner layers containing filamentous conchocelis of *P. haitanensis* were collected from the Nori cultivation base of Yingke Seaweed Cultivation Ltd. in Nanao Island (117.09° E, 23.47° N), Shantou, China, during June 2005. They were maintained in seawater pools shaded (maximal PAR under the nursing shelter ≤25 μmol photons · m^{-2} · s^{-1}, 5.5 W · m^{-2}) from direct sunlight. Sampled shells were transported in seawater within a cooler (4°C) to the laboratory in <4 h. They were maintained in filtered (Whatman GF/F; Whatman, Maidstone, UK) and sterilized seawater enriched with F medium (Guillard and Ryther 1962) at 20°C and 20 μmol photons · m^{-2} · s^{-1} of PAR (4.3 W · m^{-2}) provided by fluorescent lamps (12:12 light:dark [L:D]) in an incubator (GXZ-300D; Jiangnan Instruments Ltd., Ningbo, China) before being used for the experiments the next day.

Free-living vegetative conchocelis of *P. haitanensis* was obtained from the Laboratory of Marine Genetics and Breeding, Ocean University of China, and cultured in 500 mL flasks with the F-medium-enriched seawater, at 20°C and 20 μmol photons · m^{-2} · s^{-1} of PAR (4.3 W · m^{-2}) (Tang and Fei 1997) (12:12 L:D) in the incubator. Half of the enriched seawater in each flask was renewed every week. To avoid self-shading and maintain a homogenous culture, colonies of the conchocelis were cut into fragments of 0.5 to 1 mm in length with a sterilized household mixer and then resuspended in fresh medium and cultured for 3 d for full recovery from the mechanical injury, which immediately resulted in 60% reduction of maximal PSII photochemical efficiency after the cutting.

Radiation measurements and treatments. Indoor measurements of PAR (400–700 nm) in the illuminated incubator were carried out using an SKP-200 quantum meter (Skye Instruments Ltd., Wales, UK). A solar simulator (SOL 1200 W, Dr. Hönle AG, Munich, Germany) was used to provide simulated solar irradiance for indoor experiments. Outdoor and simulated solar radiations were measured using a broad band filter radiometer (ELDONET, Real Time Computers, Erlangen, Germany). This instrument measures irradiances every second at three wavelength bands of 400–700 nm (PAR), 315–400 nm (UVA), and 280–315 nm (UVB) and records the data (means over 60 s) at 1 min intervals in a PC (Häder et al. 1999). It has been certified as having a correspondence error <0.5% in comparison with the most accurate instrument (certificate No. 2006/BB14/1) and has been calibrated regularly with assistance from the manufacturer.

Three radiation treatments were implemented using UV-filtering foils: (1) samples exposed to PAR alone (PAR) (covered with an Ultraphan 395 filter, UV Opak; Digefra, Munich, Germany); (2) samples exposed to PAR + UVA (PA) (covered with a Folex 320 filter, Folex, Dreieich, Germany); (3) samples exposed to PAR + UVA + UVB (PAB) (covered with an Ultraphan 295 filter; Digefra). The spectra of these materials were published in Korbee Peinado et al. (2004).

Measurements of photochemical efficiency and photosynthetic carbon fixation. Photochemical efficiency or the effective quantum yield of PSII ($\Delta F/F_m'$, Genty et al. 1989) was measured using a portable pulse-amplitude-modulated fluorometer (Water-PAM; Walz, Effeltrich, Germany). For measurements in the free-living conchocelis, the Water-ED Emitter-Detector Unit was used, while for the conchocelis in the covering calcareous matrix, the Water-EDF Fiberoptics-Emitter-Detector Unit was applied with its optical fiber probe directly pointed at the conchocelis patch at 5 mm distance.

$$\Delta F/F_m' = (F_m' - F_t)/F_m' \quad (1)$$

measured with an actinic light of 300 μmol photons · m^{-2} ·s^{-1} (65.2 W · m^{-2}) under a modulated measuring light of 0.3 μmol photons · m^{-2} · s^{-1} (0.06 W · m^{-2}), and the saturating pulse was about 5,600 μmol photons · m^{-2} · s^{-1} (1,217.4 W · m^{-2}) for 0.8 s.

Photosynthetic carbon fixation was determined for the free-living conchocelis fragments (0.5–1.0 mm long). The resuspended fragments of about 9 mL were placed in a 10 mL quartz tube and inoculated with 0.1 mL–5 μCi (0.185 MBq) of labeled sodium bicarbonate ($NaH^{14}CO_3$). After 0.5–2 h incubations, the samples were filtered onto Whatman GF/F glass fiber filters (25 mm), exposed to HCl fumes in darkness overnight to expel inorganic carbon as CO_2, dried at 40°C, and then dissolved in scintillation cocktail (PerkinElmer, Shelton, CT, USA). The incorporated activity was determined using a liquid scintillation counter (LS 6500 Multi-Purpose Scintillation Counter; Beckman Coulter, Fullerton, CA, USA) (Holm-Hansen and Helbling 1995).

The relative photosynthetic inhibition (INH, %) due to UVR, UVA, or UVB was calculated as follows:

$$\mathrm{INH_{UVR}}(\%) = (\mathrm{P_{PAR}} - \mathrm{P_{PAB}})/(\mathrm{P_{PAR}}) * 100 \quad (2)$$

$$\mathrm{INH_{UVA}}(\%) = (\mathrm{P_{PAR}} - \mathrm{P_{PA}})/(\mathrm{P_{PAR}}) * 100 \quad (3)$$

$$\mathrm{INH_{UVB}}(\%) = \mathrm{INH_{UVR}}(\%) - \mathrm{INH_{UVA}}(\%) \quad (4)$$

where P_{PAR}, P_{PA}, and P_{PAB} represent the values after the exposures to PAR, PAR + UVA, and PAR + UVA + UVB, respectively.

Determination of chl a. The shells with conchocelis living in their inner layer were broken, and the conchocelis-inhabited areas were cut out and immersed in absolute methanol at 4°C for 24 h in darkness for extraction of pigments, which had been tested to result in complete extraction. After centrifugation (5804R; Eppendorf, Hamburg, Germany) at 5,000*g* for 15 min, the supernatant was scanned in a spectrophotometer (UV-2501 PC; Shimadzu, Kyoto, Japan) to obtain the spectral absorption (250–750 nm). Triplicate conchocelis-inhabited shells were used, and chl *a* density per area was determined by normalizing the chl *a* amount to the conchocelis-patch area in the shell's inner surface. Suspended fragments of free-living vegetative conchocelis were filtered onto Whatman GF/F glass fiber filters (25 mm) and then extracted in absolute methanol as above. Triplicate samples were extracted to determine the concentration of chl *a*. The chl *a* content was calculated according to Porra (2002).

Determination of the thickness and transmission spectrum of the covering calcareous matrix. The thickness of the conchocelis-sheltering layer was estimated by measuring the difference in the thickness of the shell before and after the conchocelis-sheltering layer was scraped off, to an accuracy of 0.01 mm with a micrometer. To determine how much UVR and PAR this layer would screen out for the conchocelis residing underneath, the inner layers of the shells were ground to 0.22, 0.25, and 0.32 mm thick, and their transmission spectra were determined. The transmission spectrum for the covering calcareous matrix was then derived from the differences between the above spectra according to its thickness.

To examine the protective role of the covering calcareous matrix, an artificial filter was made with two layers of polymethylmethacrylate board (UV transparent Plexiglas;

Evonik Industries, Darmstadt, Germany) and an interlayer of suntan cream (SPF18, Mininurse; Ratstar Cosmetics Co. Ltd., Shenzhen, China); this artificial filter had a similar transmission spectrum with the covering calcareous matrix (Fig. 3B). Transmission characteristics of the artificial filter were not altered after 4 h exposures to solar radiation. Free-living conchocelis was covered with this shading layer, and its photosynthetic performance was examined. Although there was a difference between the absorptions of the artificial layer and the covering calcareous matrix at wavebands shorter than 290 nm, 295 filtering foils were applied to all the samples that were exposed under the solar simulator; therefore, the simulated shading layer was suitable to reflect the transmission features of the covering calcareous matrix.

Diurnal photosynthetic performance of shell-living conchocelis. The diurnal photochemical performance of the shell-living conchocelis, as affected by solar radiation, was monitored every 60 min on May 26, 2005, at the nursing shelter (at 10–20 cm depth of seawater), with about 1.4% of the incident radiation on the surface of the pool. Five shells were picked randomly for each measurement in this experiment. In addition, some shell-living conchocelis were taken outside of the shelter and exposed to high levels of radiation by exposing them to 50% of incident solar radiation, covering them with one layer of neutral density net (stainless steel) on June 28, 2005, and the effective quantum yield was measured at 1–2 h intervals. For this latter exposure to 50% solar radiation, two shells were placed in each of 250 mL quartz tubes (5.4 cm inner diameter) with F-medium-enriched seawater (not agitated with aeration as in the nursing shelter). Different radiation treatments with or without UVR were carried out, and duplicate tubes (total four shells) were employed for each treatment.

Physiological function of the covering calcareous matrix. To test to what extent the covering calcareous matrix protects the shell-living conchocelis, we used free-living conchocelis that were sheltered or not with the artificial sheltering film. Homogeneous suspended fragments of the conchocelis were exposed under the solar simulator with or without being shaded with the artificial film, and both the effective quantum yield and photosynthetic carbon fixation were measured. Both treatments were exposed to the same radiation levels, but due to the attenuation of the artificial sheltering film, the irradiances received by the cells were different. The free-living conchocelis received 118 $W \cdot m^{-2}$ PAR (543 μmol photons $\cdot m^{-2} \cdot s^{-1}$), 25.5 $W \cdot m^{-2}$ UVA, and 1.15 $W \cdot m^{-2}$ UVB, while the shaded conchocelis received 77 $W \cdot m^{-2}$ PAR (354 μmol photons $\cdot m^{-2} \cdot s^{-1}$), 11.7 $W \cdot m^{-2}$ UVA, and 0.32 $W \cdot m^{-2}$ UVB. The biologically weighted UVB irradiances for both conditions were 0.11 and 0.03 $W \cdot m^{-2}$, respectively (Setlow 1974, normalized to 1.0 at 300 nm).

The effective quantum yield was measured on fragments of the free-living conchocelis (at the same chl *a* density per area with that in the shell at 5.74 ± 0.17 μg chl $a \cdot cm^{-2}$) that were exposed (1 h) to PAR, PA, and PAB in open petri dishes (inner diameter 86 mm, height 17 mm) with 60 mL F-medium-enriched seawater (shaken every 15 min). For the determination of photosynthetic carbon fixation, suspended conchocelis fragments were diluted with the medium to 32 μg chl $a \cdot L^{-1}$ before being used. All samples were exposed to PAB treatment, and triplicate incubations were carried out for each determination after 0.5, 1, and 1.5 h periods, to determine carbon incorporation under full spectrum of solar radiation as a function of incubation time.

In the above experiments, the cells under the sheltering film received less PAR and UVR than those that were nonshaded. It was still difficult to distinguish the protective role against UVR played by the sheltering layer due to the difference in PAR between the covered and noncovered treatments. Therefore, we reduced the solar radiation for the nonsheltered cells by covering them with one layer of neutral density net, so that the cells received the same amount of PAR with 19% more UVA and 37% more UVB as compared with those under the artificial shading filter. The PAR irradiances reaching the free-living conchocelis were regulated to be 10, 20, 45, 75, and 120 μmol photons $\cdot m^{-2} \cdot s^{-1}$ (2.2, 4.3, 9.8, 16.3 and 26.1 $W \cdot m^{-2}$, respectively) by adjusting the distance from the xenon lamp to the samples, and such PAR levels were supported by Zheng et al. (1980) and Chen et al. (1984). The ratio of PAR:UVA:UVB was 100:20.8:1.10, with the ratio of UVB to PAR ~40%–100% higher than that of the local solar radiation at noon. The actual irradiances of PAR, UVA, and UVB received by the cells are listed in Table 1; all samples were exposed only to the full spectrum of the lamp (i.e., PAB treatment) as they received the same levels of PAR, but different UVR. This allowed us to establish the protective role of the covering calcareous matrix as a function to different UVR levels. At 120 μmol photons $\cdot m^{-2} \cdot s^{-1}$ of PAR, DNA-weighted UVB irradiance was 0.04 $W \cdot m^{-2}$ for samples covered by the neutral density net and 0.01 $W \cdot m^{-2}$ for samples covered by the simulated shading layer. The suspended conchocelis fragments were diluted with the medium to final concentration of 142 μg chl $a \cdot L^{-1}$. All samples were placed in 10 mL quartz tubes with half of them inoculated with $NaH^{14}CO_3$. At variable time after exposure (i.e., 0.5, 1, 1.5, and 2 h), triplicate samples inoculated with $NaH^{14}CO_3$ either under the simulated shading layer or the neutral density net were taken to measure carbon fixation. At the same time, the effective quantum yield was determined in another set of triplicate samples that were not inoculated with the isotope. The quartz tubes were shaken slightly every 15 min during the incubation. The temperature under the solar simulator was controlled at 23°C–25°C by cooling air or at 22°C–26°C for outdoor incubations in a flow-through water bath.

Table 1. Irradiances of UVA and UVB received by samples covered with one layer of neutral density net (65% transmission) or with the simulated shading layer at the same PAR levels.

PAR (μmol photons $\cdot m^{-2} \cdot s^{-1}$)	UVA ($W \cdot m^{-2}$)	UVB ($W \cdot m^{-2}$)
10	0.5 (0.3)	0.02 (0.01)
20	0.9 (0.6)	0.05 (0.02)
45	2.0 (1.4)	0.11 (0.04)
75	3.4 (2.4)	0.18 (0.08)
120	5.4 (3.8)	0.29 (0.13)

Data in the parentheses represent the irradiances under the simulated shading layer.

Statistics. In all experiments, triplicate samples were used for each treatment, and the data were expressed as mean ± standard deviation (n = 3–6). Statistical significance among different treatments was tested with *t*-test or one-way analysis of variance (ANOVA) at a significance level of $P < 0.05$. Tukey's post hoc test was applied for comparison of means for the ANOVA.

RESULTS

Diurnal photochemical performance of shell-living conchocelis. Maximal irradiances under the nursing shelter were 4.52 $W \cdot m^{-2}$ for PAR (18.98 μmol photons $\cdot m^{-2} \cdot s^{-1}$), 0.27 $W \cdot m^{-2}$ for UVA, and 0.01 $W \cdot m^{-2}$ for UVB on May 26, 2005, when outside direct solar PAR was about 100 times higher (Fig. 1A, outside irradiances not shown). The

effective quantum yield of *P. haitanensis* conchocelis in the shell was inversely correlated with irradiance, starting with a value of 0.68 in the early morning, decreasing to 0.47 ($P < 0.05$, *t*-test) at the midday, and then increasing in the late afternoon to the same level as in the early morning (Fig. 1B). On June 28, 2005, the shells were exposed to 50% of the incident solar radiation that had maximal irradiances of 448 $W \cdot m^{-2}$ for PAR (2,061 μmol photons $\cdot m^{-2} \cdot s^{-1}$), 80 $W \cdot m^{-2}$ for UVA, and 1.88 $W \cdot m^{-2}$ for UVB) (Fig. 2A). Under these conditions, photosynthesis was significantly impacted by solar radiation, and the yield decreased sharply to 32% (PAR), 16% (PA, PAR + UVA), and 11% (PAB, PAR + UVA + UVB) of the initial value (0.61) ($P < 0.05$, *t*-test) after 1 h of exposure, and to 2% (PAR), 1% (PA), and 0.2% (PAB) after 4 h of exposure, respectively (Fig. 2B). The bulk of the inhibition and thus the reduced yield was due to PAR (about 87%). UVR induced additional reduction of the yield of 13%, of which UVA and UVB accounted for 9% and 4% ($P < 0.05$, one-way ANOVA, $F_{2,10}$), respectively. No recovery was observed in the afternoon when solar radiation decreased.

Transmission spectrum of the covering calcareous matrix. The spectral characteristics of the *P. haitanensis* conchocelis are shown in Figure 3A. There was a small absorption peak for UV-absorbing compounds (absorbance between 310 and 360 nm), together with the obvious peaks for chl *a* and carotenoid. The thickness of the covering calcareous matrix that shelters the conchocelis was determined to be 0.06 ± 0.01 mm ($n = 5$, five shells). The 0.06 mm thick covering calcareous matrix reduced 30%–45% of PAR, 50%–60% of UVA, and 60%–80% of UVB in terms of their transmissions (Fig. 3B). The average transmission of the 0.06 mm covering calcareous matrix was 63% for PAR, 47% for UVA, and 36% for UVB, respectively, and that of the simulated shading layer was 65%, 46%, and 28%, respectively.

Photoprotection of the covering calcareous matrix under high PAR and/or UVR. To assess the photoprotection of the covering calcareous matrix, incubations were performed using *P. haitanensis* free-living conchocelis that were covered with or without the artificial simulated shading layer (spectra in Fig. 3B). The samples were exposed to simulated solar radiation of 118 $W \cdot m^{-2}$ PAR (543 μmol photons $\cdot m^{-2} \cdot s^{-1}$), 25.5 $W \cdot m^{-2}$ of UVA, and 1.15 $W \cdot m^{-2}$ of UVB. The artificial shading layer reduced the PAR, UVA, and UVB irradiances by 35, 54, and

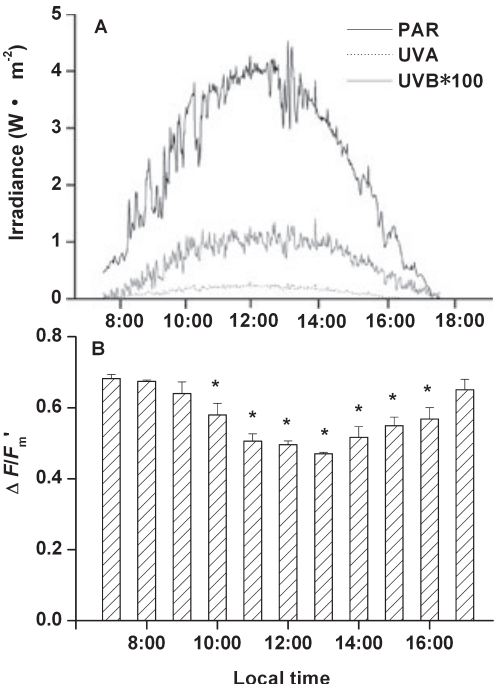

FIG. 1. (A) Irradiances of solar PAR, UVA, and UVB*100 ($W \cdot m^{-2}$) on May 26, 2005, under the sheltered nursing base for *Porphyra haitanensis* shell-living conchocelis. (B) Effective quantum yield of the shell-living conchocelis measured at hourly intervals during the daytime. Data are the means ± SD for five different shells ($n = 5$). Significant difference from the initial value was indicated as "*". UVA, ultraviolet radiation A; UVB, ultraviolet radiation B.

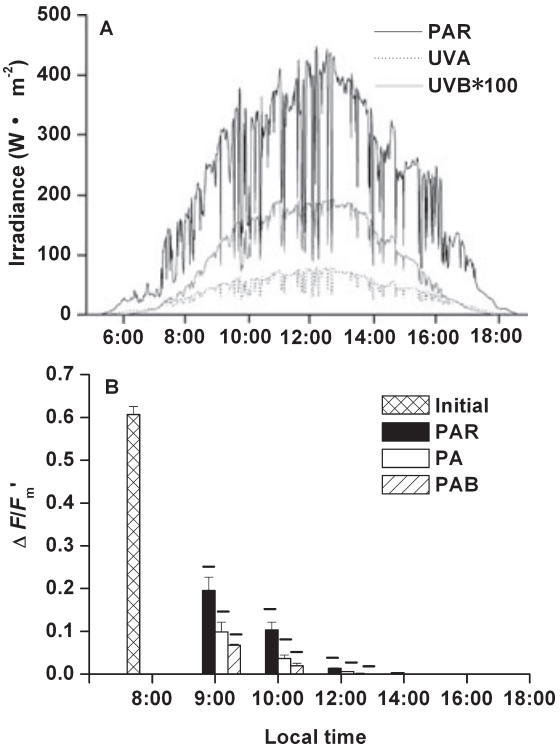

FIG. 2. *Porphyra haitanensis* shell-living conchocelis was exposed to 50% of the incident solar radiation (A) under PAR, PAR + UVA (PA), or PAR + UVA + UVB (PAB) on June 28, 2005, and the effective quantum yield was measured at irregular intervals (B). Data are mean ± SD for six shells ($n = 6$). Horizontal lines over the histograms indicate significant differences among the radiation treatments. UVA, ultraviolet radiation A; UVB, ultraviolet radiation B.

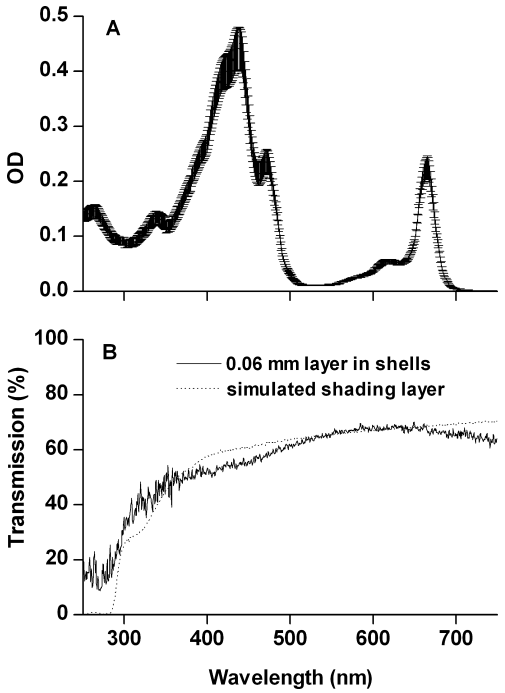

FIG. 3. (A) Absorption characteristics of the extract from *Porphyra haitanensis* shell-living conchocelis. Data are mean ± SD ($n = 3$). (B) Spectral transmission of 0.06 mm thick covering calcareous matrix and the simulated shading foil. OD, optical density.

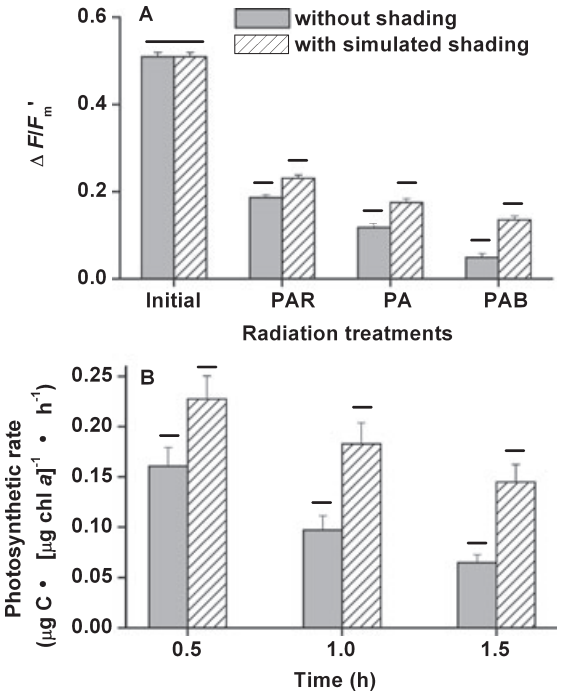

FIG. 4. Free-living conchocelis of *Porphyra haitanensis* was covered by the artificial shading layer or directly exposed to the simulated solar radiation (543 μmol photons · m^{-2} · s^{-1} PAR, 25.5 W · m^{-2} UVA, and 1.15 W · m^{-2} UVB). (A) Effective quantum yield of samples under PAR, PAR + UVA (PA), and PAR + UVA + UVB (PAB), respectively. Data are mean ± SD ($n = 6$). (B) Photosynthetic carbon fixation rates of samples under PAR + UVA + UVB treatment for 0.5–1.5 h. Data are mean ± SD ($n = 3$). Horizontal lines over the histograms indicate significant differences between samples with and without the simulated layer. UVA, ultraviolet radiation A; UVB, ultraviolet radiation B.

72%, respectively, thus resulting in lower irradiances received by the cells under the shading layer. After 1 h of exposure, the effective quantum yield decreased significantly ($P < 0.05$, *t*-test) to 37% (PAR), 23% (PA), and 10% (PAB) in the samples not covered with the simulated shading layer and to 45% (PAR), 34% (PA), and 27% (PAB) of the initial value (0.51) in those maintained under it (Fig. 4A), reflecting that the simulated shading layer led to much less photoinhibition caused by PAR and/or UVR. In contrast to PAR treatment, the relative inhibition caused by UVR was ~41% (UVA 24%, UVB 17%, *t*-test) in samples under the simulated shading and was higher in samples without shading, reaching 74% (UVA 37%, UVB 37%, *t*-test). When the photosynthetic carbon fixation (Fig. 4B) was determined under the full spectrum of solar radiation, the presence of the simulated shading layer resulted in higher photosynthetic rates ($P < 0.05$, *t*-test) by 42% in 0.5 h, 89% in 1 h, and 124% in 1.5 h, respectively, as compared with the rates in the uncovered samples.

Additionally, when the free-living conchocelis was exposed to the same PAR levels of 10–120 μmol photons · m^{-2} · s^{-1} (2.2–26.1 W · m^{-2}), but to different levels of UVR (variation in UVR was achieved by covering some samples with neutral screens to reduce equally the energy of all wavelengths or with the artificial shading layer that screened out more UVR), the simulated shading layer exhibited a significant protective role against UVR. At 45 μmol photons · m^{-2} · s^{-1} of PAR (9.8 W · m^{-2}) and above, there was a significant decrease in the effective quantum yield with exposure time (Fig. 5). Throughout the experimental period, the yield showed no significant difference among the treatments at PAR levels of 10, 20, and 45 μmol photons · m^{-2} · s^{-1} (2.2, 4.3, 9.8 W · m^{-2}, respectively) ($P > 0.05$, *t*-test) (Fig. 5, A–C). The inhibition of the yield, however, was significantly higher ($P < 0.05$, *t*-test) in cells exposed to PAR levels of 75 and 120 μmol photons · m^{-2} · s^{-1} (16.3 and 26.1 W · m^{-2}) under the neutral density net than under the artificial layer (Fig. 5, D and E), under which the yield was 44% and 77% higher than that under the neutral screen at the corresponding PAR levels, respectively.

In terms of the photosynthetic carbon fixation (Fig. 6), the rate of carbon fixation did not show significant differences ($P > 0.05$) between the two kinds of sheltering at PAR levels of 75 μmol photons · m^{-2} · s^{-1} (16.3 W · m^{-2}) or lower (Fig. 6, A–D). At the PAR level of 120 μmol photons · m^{-2} · s^{-1} (26.1 W · m^{-2}), however, a significant difference was evident between the two kinds of

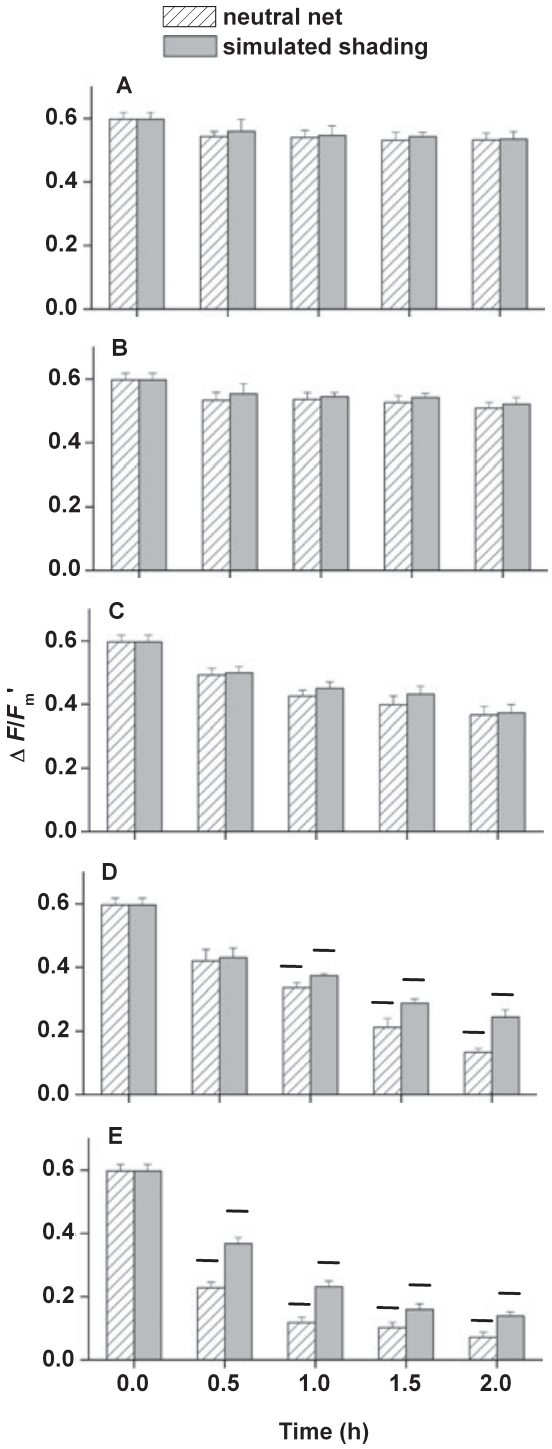

FIG. 5. Effective quantum yield of the free-living conchocelis of *Porphyra haitanensis* under one layer of neutral density net or the simulated shading layer exposed to the simulated solar radiation under PAR + UVA + UVB treatment for 0.5–2 h. The actual PAR irradiances received by the samples were 10 μmol photons · m^{-2} · s^{-1} (A), 20 μmol photons · m^{-2} · s^{-1} (B), 45 μmol photons · m^{-2} · s^{-1} (C), 75 μmol photons · m^{-2} · s^{-1} (D), 120 μmol photons · m^{-2} · s^{-1} (E), respectively. Data are means ± SD (n = 6). Horizontal lines over the histograms indicate significant differences between samples covered with neutral density net and with the simulated shading layer. UVA, ultraviolet radiation A; UVB, ultraviolet radiation B.

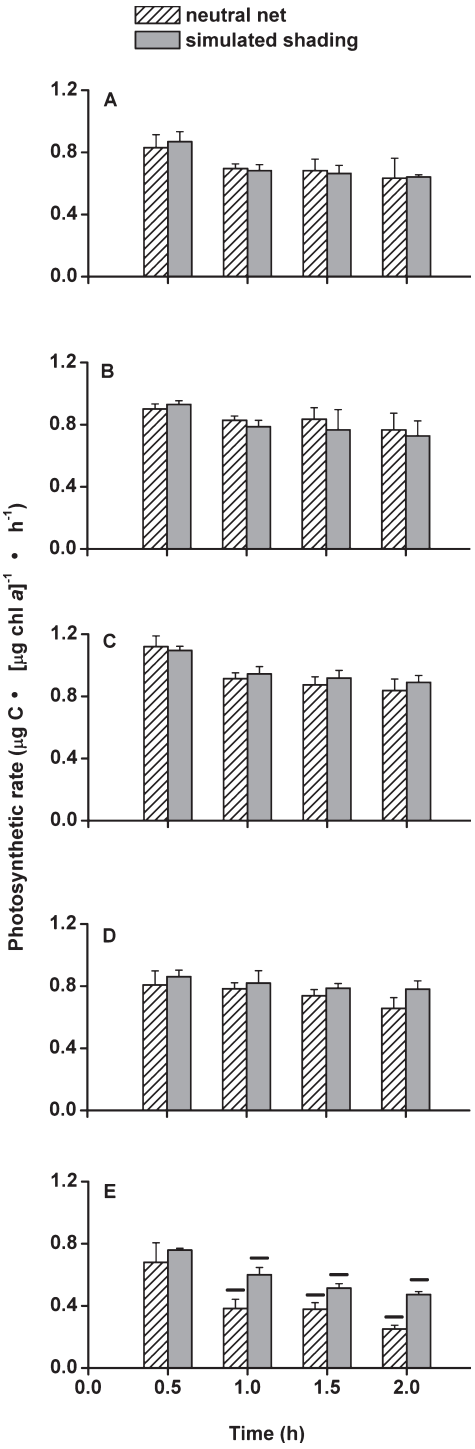

FIG. 6. Photosynthetic carbon fixation rates of the free-living conchocelis of *Porphyra haitanensis* under one layer of neutral density net or the simulated shading layer exposed to the simulated solar radiation under PAR + UVA + UVB treatment for 0.5–2 h. The actual PAR irradiances received by the samples were 10 μmol photons · m^{-2} · s^{-1} (A), 20 μmol photons · m^{-2} · s^{-1} (B), 45 μmol photons · m^{-2} · s^{-1} (C), 75 μmol photons · m^{-2} · s^{-1} (D), 120 μmol photons · m^{-2} · s^{-1} (E), respectively. Data are means ± SD (n = 3). Horizontal lines over the histograms indicate significant differences between samples covered with neutral density net and with the simulated shading layer. UVA, ultraviolet radiation A; UVB, ultraviolet radiation B.

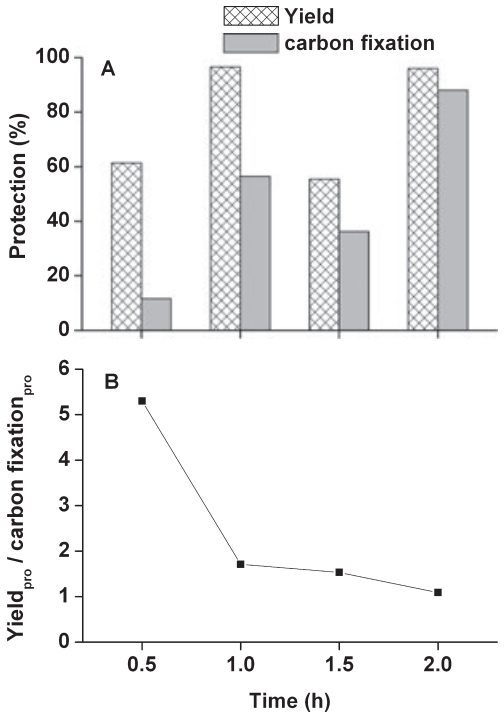

FIG. 7. Free-living conchocelis of *Porphyra haitanensis* were exposed to the simulated solar radiation under PAR + UVA + UVB treatment for 0.5–2 h and received real PAR of 120 μmol photons · m^{-2} · s^{-1}. (A) Protection of the effective quantum yield and carbon fixation rates due to the simulated shading layer. (B) Ratio of protection of the effective quantum yield (yield$_{pro}$) to that of carbon fixation rates (carbon fixation$_{pro}$). UVA, ultraviolet radiation A; UVB, ultraviolet radiation B.

shading after 1 h of exposure. The photosynthetic carbon fixation rate was ~60% higher in the cells covered with the simulated shading layer than in the cells under the neutral screen ($P < 0.05$, *t*-test) (Fig. 6E), which also reflected a protective role played by the covering calcareous matrix for the conchocelis. Nevertheless, the highest rate of carbon fixation was always found at 45 μmol photons · m^{-2} · s^{-1} PAR (9.8 W · m^{-2}).

We used the data of Figures 5 and 6 to compare the level of protection, between the artificial and the neutral density nets, in terms of the effective quantum yield and carbon fixation rates at PAR of 120 μmol photons · m^{-2} · s^{-1} (26.1 W · m^{-2}) (Fig. 7A). The artificial shading layer provided more protection to the effective quantum yield than to the photosynthetic carbon fixation (Fig. 7A). As indicated in the ratio of the protection of the yield to that of the carbon fixation (Fig. 7B), dark reactions of photosynthesis in the conchocelis were less protected during the exposure but reached almost similar values (ratio of 1) with the light reactions after 2 h.

DISCUSSION

The intertidal-inhabited thalli of *P. haitanensis* were previously determined to contain a higher amount of UV-absorbing compounds than the conchocelis stage, resulting in less inhibition caused by UVR (Jiang et al. 2008). The UV-absorbing compounds, mainly MAAs, are known to be able to screen out harmful radiation within the UV wavebands (Karsten et al. 1998). Since the conchocelis stage of *P. haitanensis* contained very little of these compounds (Fig. 3A), ~1%–2% of the thallus stage (Jiang and Gao 2008), it lacks efficient defensive capability against UVR. Exposure to solar UVR showed no induction of UV-absorbing compounds (data not shown). Alternatively, the conchocelis residing in the covering calcareous matrix can avoid harmful solar radiation to a considerable extent, since the covering calcareous matrix can reduce 64% UVB, 53% UVA, and 37% PAR (Fig. 3B).

Most of the observed inhibition of photochemical efficiency in *P. haitanensis* conchocelis in shells was caused by PAR (Fig. 2B). The inner layer of the shell that shelters the conchocelis transmits more PAR than UVR (Fig. 3B), and PAR represents the highest proportion in the whole spectrum of solar radiation. Previous studies also showed that the conchocelis of *Porphyra* plants was highly sensitive to high levels of PAR (Jiang and Gao 2008, Lin et al. 2008). Nevertheless, UVR still caused significant additional inhibition of photosynthesis, although its transmission was largely reduced by the covering calcareous matrix.

The protection provided by the covering calcareous matrix for the free-living conchocelis under both high PAR and UVR was significant in view of photochemical efficiency and photosynthetic carbon fixation (Figs. 4 and 7). Not only could the light levels be lowered, but the light quality was also changed; therefore, this layer screened out relatively more (percentage-wise) UVR than PAR and resulted in efficient reduction of UV-related inhibition of photosynthesis. Higher ratios of UVB to UVA and PAR led to more reduction in maximal quantum yield in the thalli of *Porphyra leucosticta* and *P. umbilicalis* (Korbee et al. 2005); reduction in such ratios by the covering calcareous matrix must have protected the photosynthetic apparatus of *P. haitanensis* conchocelis.

The protection by the covering calcareous matrix within the UVR range was obvious at PAR levels of 75 and 120 μmol photons · m^{-2} · s^{-1} (16.3 and 26.1 W · m^{-2}) (Figs. 5 and 6). Carbon fixation was reported to be more susceptible to UVB damage than PSII efficiency (Franklin et al. 2003). In the present study, we determined that the covering calcareous matrix did provide more protection to PSII photochemistry than to carbon fixation (Fig. 7B). The thickness of the covering calcareous matrix can vary according to species and environmental conditions. It was reported that *Porphyra* conchocelis resided deeper in the shell under higher irradiances (Zhang 1988). We have shown here that the covering calcareous matrix provided significant

protection for PSII activity and carbon fixation in *P. haitanensis* conchocelis. The phenomenon that the conchocelis stage of *Porphyra* plants resides in shells' inner layer (Drew 1949) can be considered to be a strategy to avoid harmful solar UVR during the summer period. Fossils of putative *Porphyra* conchocelis named *Palaeoconchocelis* have been aged 425 million years (Campbell 1980), when solar UV radiation was much stronger than today (Cockell 2001). Shelled marine invertebrates might have provided potential habitats for the *Porphyra* conchocelis to occupy (Stiller and Waaland 1993). In culture, conchocelis growth and reproduction do not require a calcareous substratum; however, they do in nature. *P. abbottiae* conchocelis burrowed deeper in shells when exposed to higher levels of light (Lin et al. 2008). Escaping from high solar radiation by burrowing in the calcarious matrix could be a strategy for the conchocelis to survive.

This study was funded by ''863'' project (2006AA10A413) from Ministry of Science and Technology, National Natural Science Foundation of China (Key Project No. 90411018) and Science Foundation of Changshu Institute of Technology (No. KY11707). We acknowledge Yingke Seaweed Cultivation Ltd. in Nanao Island for providing *P. haitanensis* conchocelis in shells, and Xiaorong Tang for providing free-living conchocelis of *P. haitanensis*. We thank Zengling Ma, Gang Li, and Yaping Wu for experimental assistance and Weizhou Chen for his kind support during the stay at the marine biology station.

Campbell, S. E. 1980. *Palaeoconchocelis starmachii*, a carbonate boring microfossil from the Upper Silurian of Poland (425 million years old): implications for the evolution of the Bangiaceae (Rhodophyta). *Phycologia* 19:25–36.

Chen, G., Zhang, X., Zhou, H. & Zhang, J. 1984. The effect of some ecological factor on the photosynthetic activity of free-living filaments in early stage of *Porphyra haitanensis*. *J. Fish. China* 8:115–23.

Cockell, C. 2001. A photobiological history of Earth. *In* Cockell, C. & Blaustein, A. R. [Eds.] *Ecosystems, Evolution, and Ultraviolet Radiation*. Springer Verlag, New York, pp. 1–35.

Coelho, S. M., Rijstenbil, J. W., Sousa-Pinto, I. & Brown, M. T. 2001. Cellular responses to elevated light levels in *Fucus spiralis* embryos during the first days after fertilization. *Plant Cell Environ.* 24:801–10.

Cole, K. M. & Conway, E. 1980. Studies in the Bangiaceae: reproductive modes. *Bot. Mar.* 23:545–53.

Drew, K. M. 1949. Conchocelis-phase in the life-history of *Porphyra umbilicalis* (L.) Kütz. *Nature* 164:748–9.

Dring, M. J., Makarov, V., Schoschina, E., Lorenz, M. & Lüning, K. 1996. Influence of ultraviolet-radiation on chlorophyll fluorescence and growth in different life-history stages of three species of *Laminaria* (Phaeophyta). *Mar. Biol.* 126:183–91.

Fairhead, V. A., Amsler, C. D. & McClintock, J. B. 2006. Lack of defense or phlorotannin induction by UV radiation or mesograzers in *Desmarestia anceps* and *D. menziesii* (Phaeophyceae). *J. Phycol.* 42:1174–83.

Franklin, L. A., Osmond, C. B. & Larkum, A. W. D. 2003. Photoinhibition, UV-B and algal photosynthesis. *In* Larkum, A. W. D., Douglas, S. E. & Raven, J. A. [Eds.] *Photosynthesis in Algae*. Kluwer Academic Publishers, Dordrecht, the Netherlands, pp. 351–84.

Genty, B., Briantais, J. M. & Baker, N. R. 1989. The relationship between the quantum yield of photosynthetic electron transport and quenching of chlorophyll fluorescence. *Biochim. Biophys. Acta* 990:87–92.

Guillard, R. R. L. & Ryther, J. H. 1962. Studies of marine planktonic diatoms. I. *Cyclotella nana* Hustedt and *Detonula confervacea* (Cleve) Gran. *Can. J. Microbiol.* 8:229–39.

Häder, D.-P., Lebert, M., Marangoni, R. & Colombetti, G. 1999. ELDONET-European Light Dosimeter Network hardware and software. *J. Photochem. Photobiol. B Biol.* 52:51–8.

Hawkes, M. W. 1978. Sexual reproduction in *Porphyra gardneri* (Smith *et* Hollenberg) Hawkes (Bangiales, Rhodophyta). *Phycologia* 17:329–53.

Holm-Hansen, O. & Helbling, E. W. 1995. Técnicas para la medición de la productividad primaria en el fitoplancton. *In* Alveal, K., Ferrario, M. E., Oliveira, E. C. & Sar, E. [Eds.] *Manual de Métodos Ficológicos*. Universidad de Concepción, Concepción, Chile, pp. 329–50.

Jiang, H. & Gao, K. 2008. Effects of UV radiation on the photosynthesis of conchocelis of *Porphyra haitanensis* (Bangiales, Rhodophyta). *Phycologia* 47:241–8.

Jiang, H., Gao, K. & Helbling, E. W. 2008. UV-absorbing compounds in *Porphyra haitanensis* (Rhodophyta) with special reference to effects of desiccation. *J. Appl. Phycol.* 20:387–95.

Karsten, U., Franklin, L. A., Lüning, K. & Wiencke, C. 1998. Natural ultraviolet radiation and photosynthetically active radiation induce formation of mycosporine-like amino acids in the marine macroalga *Chondrus crispus* (Rhodophyta). *Planta* 205:257–62.

Korbee, N., Huovinen, P., Figueroa, F. L., Aguilera, J. & Karsten, U. 2005. Availability of ammonium influences photosynthesis and the accumulation of mycosporine-like amino acids in two *Porphyra* species (Bangiales, Rhodophyta). *Mar. Biol.* 146: 645–54.

Korbee Peinado, N., Abdala Díaz, R. T., Figueroa, F. L. & Helbling, E. W. 2004. Ammonium and UVR stimulate the accumulation of mycosporine-like amino acids (MAAs) in *Porphyra columbina* (Rhodophyta) from Patagonia, Argentina. *J. Phycol.* 40:248–59.

Lin, R., Lindstrom, S. C. & Stekoll, M. S. 2008. Photosynthesis and respiration of the conchocelis stage of Alaskan *Porphyra* (Bangiales, Rhodophyta) species in response to environmental variables. *J. Phycol.* 44:573–83.

Lud, D., Buma, A. G. J., van de Poll, W., Moerdijk, T. C. W. & Huiskes, A. H. L. 2001. DNA damage and photosynthetic performance in the Antarctic terrestrial alga *Prasiola crispa* ssp. *antarctica* (Chlorophyta) under manipulated UV-B radiation. *J. Phycol.* 37:459–67.

Pakker, H., Beekman, C. A. C. & Breeman, A. M. 2000. Efficient photoreactivation of UVBR-induced DNA damage in the sublittoral macroalga *Rhodymenia pseudopalmata* (Rhodophyta). *Eur. J. Phycol.* 35:109–14.

Porra, R. J. 2002. The chequered history of the development and use of simultaneous equations for the accurate determination of chlorophylls *a* and *b*. *Photosynth. Res.* 73:149–56.

Setlow, R. B. 1974. The wavelengths in sunlight effective in producing skin cancer: a theoretical analysis. *Proc. Natl. Acad. Sci. U. S. A.* 71:3363–6.

Stiller, J. W. & Waaland, J. R. 1993. Molecular analysis reveals cryptic diversity in *Porphyra* (Rhodophyta). *J. Phycol.* 29: 506–17.

Tang, X. & Fei, X. 1997. The relationship between light, temperature and growth, development of free-living conchocelis of *Porphyra haitanensis*. *Oceanol. Limnol. Sin.* 28:475–82.

Zhang, Y. 1988. *Porphyra Cultivation*. China Agricultural Press, Beijing, China, 22 pp.

Zheng, B., Chen, M. & Fei, X. 1980. Effect of light on the growth and development of conchocelis of *Porphyra yezoensis*. *Oceanol. Limnol. Sin.* 11:360–8.